Effect of strain and tetragonal lattice distortions in doped perovskite manganites

Yafeng Lu,[1,2] J. Klein,[1] F. Herbstritt,[1] J. B. Philipp,[1] A. Marx,[1] and R. Gross[1]
[1]*Walther-Meißner-Institut, Bayerische Akademie der Wissenschaften, Walther-Meißner Strasse 8, D-85748 Garching, Germany*
[2]*Northwest Institute for Nonferrous Metal Research, P.O. Box 51, Xi'an, Shaanxi 710016, People's Republic of China*
(Received 31 August 2005; revised manuscript received 21 February 2006; published 5 May 2006)

A series of high-quality, coherently strained $[La_{2/3}(Ca \text{ or } Ba)_{1/3}MnO_3/SrTiO_3]\times N$ superlattices has been prepared on (100) $SrTiO_3$ and $NdGaO_3$ substrates by laser molecular beam epitaxy. The manganite layers are biaxially strained due to lattice mismatch. A quadratic decrease of the metal-to-insulator transition temperature T_p with increasing biaxial distortion ε_{bi}^2 both for tensile and compressive in-plane strain is found. For $T>T_p$, the resistivity versus temperature curves could be well described by the small polaron hopping model with the polaron binding energy increasing with increasing ε_{bi}^2. Furthermore, the magnetoresistance of the manganite films was found to strongly increase with increasing ε_{bi}^2 or decreasing T_p, respectively, following a universal behavior. An anomalous upturn of resistivity in the low-temperature regime ($T<25$ K) was detected, which may be attributed to enhanced Coulomb interaction of the charge carriers resulting from disorder due to the lattice distortion. Our analysis clearly demonstrates the importance of biaxial strain and Jahn-Teller-type lattice distortions for the physics of the doped manganites. It is shown that epitaxial coherency strain can be used to deliberately modify the materials properties.

DOI: 10.1103/PhysRevB.73.184406 PACS number(s): 75.47.Lx, 68.55.−a, 75.70.Cn

I. INTRODUCTION

Since the discovery of the colossal magnetoresistance (CMR) in epitaxial thin films of the doped perovskite manganites,[1,2] the structural and magnetotransport properties of the CMR materials have been studied intensively. In particular, much attention has been paid to the properties of thin films due to their application in both the study of the mechanism of CMR and potential magnetoelectronic devices. It became evident that there is a pronounced difference in the magnetotransport properties of thin films and bulk materials. Besides sample imperfections these differences have been attributed to substrate-induced biaxial strain in the thin-film structures due to lattice mismatch. For the physics of the CMR manganites, the strong electron lattice coupling[3] is known to play a key role as, e.g., demonstrated by the oxygen isotope effect.[4] One particular mechanism for this coupling is the Jahn-Teller (JT) effect lifting the degeneracy of the Mn e_g levels in a cubic environment by a biaxial distortion.[3] Along this line, the effect of a biaxial distortion induced by substrate strain is expected to be fundamentally different from the effect of bulk (compressive) strain driving the lattice towards cubic symmetry and to strongly affect the subtle interplay between spin, charge, structural, and orbital degrees of freedom. Therefore, the clarification of the detailed role of biaxial strain is essential and has been recently addressed in several experimental studies based on ultrathin films[5–26]and artificial heterostructures.[27–30] Beyond the influence of strain on the magnetotransport properties of the doped manganites, strain also has been found to significantly affect the noise properties. It was found that the low-frequency $1/f$ noise in strained films is drastically enhanced compared to the noise in almost strain-free films.[31–38]

The commonly applied method for the experimental study of biaxial strain effects is the growth of epitaxial thin films on single-crystalline substrates with a certain lattice mismatch, with the thickness of these films varying over a relatively large range. However, the coherently strained state can be kept only up to a critical thickness h_c, which can be estimated from continuum theory based on the elastic constants of the involved materials.[39] Increasing the film thickness above the critical thickness h_c results in a (partial) strain release accompanied by the formation of misfit dislocations and structural disorder. Even for ultrathin films of the doped manganites the strain distribution can be inhomogeneous across growth islands.[40,41] Therefore, in general it is difficult to separate intrinsic strain effects from other extrinsic factors for CMR single-layer films.

In this paper we present a detailed study of epitaxial $La_{2/3}Ba_{1/3}MnO_3$ (LBMO) and $La_{2/3}Ca_{1/3}MnO_3$ (LCMO) thin films under tensile and compressive biaxial strain, respectively. The strain and the resulting tetragonal lattice distortion has been varied over a wide range by preparing a series of $[La_{2/3}(Ca \text{ or } Ba)_{1/3}MnO_3/SrTiO_3]\times N$ superlattices with different modulation periods on (100) $SrTiO_3$ (STO) and $NdGaO_3$ (NGO) substrates using UHV-laser molecular beam epitaxy (L-MBE).[42] We show that the insulator-to-metal transition temperature T_p decreases strongly with increasing biaxial distortion ε_{bi} both for tensile and compressive strain with $\Delta=1/T_p d^2T_p/d\varepsilon_{bi}^2$ (note that $dT_p/d\varepsilon_{bi}=0$ by symmetry reasons) being similar for tensile and compressive strain. We further show that the transport for $T>T_p$ is by small polaron hopping[43–46] with the polaron trapping energy increasing with increasing biaxial distortion. In general, our results show that epitaxial coherency strain can be used to deliberately modify the magnetotransport properties of the doped manganites. This is similar to the strain modification of the properties of various ferroelectric[47–50] or superconducting[51,52] transition metal oxide films.

II. EXPERIMENT

We have used an UHV-laser molecular beam epitaxy (L-MBE) system for the deposition of the

$[La_{2/3}Ba_{1/3}MnO_3/SrTiO_3]_N$ and $[La_{2/3}Ca_{1/3}MnO_3/SrTiO_3]_N$ multilayer structures on single-crystalline substrates of $SrTiO_3(100)$ and $NdGaO_3(100)$. The UHV L-MBE system we developed for the molecular layer epitaxy of transition metal oxides has been described in detail elsewhere.[42] The substrate holder can be heated well above 1000 °C and furthermore can be rotated and tilt to allow for rocking reflection high-energy electron diffraction (RHEED). The high-pressure RHEED system allowing for the monitoring of the epitaxial growth operates up to an oxygen pressure of about 50 Pa, as has been described in detail elsewhere.[53,54] The epitaxial $[La_{2/3}Ba_{1/3}MnO_3/SrTiO_3]_N$ and $[La_{2/3}Ca_{1/3}MnO_3/SrTiO_3]_N$ heterostructures have been deposited on (100) $NdGaO_3$ and (100) $SrTiO_3$ substrates using a laser energy density of 1.2 J/cm^2 and a pulse repetition rate of 2 to 5 Hz. The substrate was kept at 760 °C and the oxygen pressure at 200 mTorr for $La_{2/3}Ba_{1/3}MnO_3$ and 150 mTorr for $SrTiO_3$, respectively, during the deposition. After the deposition, the samples were annealed *in situ* at 600 °C in 500 Torr pure oxygen for 2 h in order to obtain optimum oxygen stoichiometry. For the multilayer films the number of laser pulses used for ablation from each target was adjusted to deposit alternating layers of thickness d_1 ($SrTiO_3$) and d_2 ($La_{2/3}Ca_{1/3}MnO_3$ or $La_{2/3}Ba_{1/3}MnO_3$). The process was repeated for N cycles, starting with $SrTiO_3$ and ending with $La_{2/3}Ca_{1/3}MnO_3$ or $La_{2/3}Ba_{1/3}MnO_3$ to get multilayer structures of $[SrTiO_3(d_1\text{nm})/La_{2/3}Ca_{1/3}MnO_3$ or $La_{2/3}Ba_{1/3}MnO_3(d_2\text{nm})]_N$. The layer thickness d_1 and d_2 as well as the number N of stacked double layers (number of modulation periods) are listed in Table I. The total thickness of multilayers is less than 140 nm.

For the structural analysis of the $La_{2/3}$(Ca or Ba)$_{1/3}MnO_3/SrTiO_3$ heterostructures, both high-resolution transmission electron microscopy (HRTEM) and x-ray diffraction have been used. High-angle x-ray diffraction (HAXRD), low-angle x-ray reflectivity (LAXRR), and rocking curve measurements have been performed to get information on the structural coherency of interfaces in these superlattices.

A standard four-probe method was used to measure the electrical transport properties of the multilayer films. The preparation process of microbridges using optical lithography and Ar ion beam etching has been reported elsewhere.[27] The transport properties were measured in an Oxford variable-temperature cryostat system equipped with a 10 T superconducting solenoid.

III. RESULTS AND DISCUSSION

The thickness d_1 and d_2 of the constituent STO and LBMO/LCMO layers, respectively, as well as the number N of modulation periods of the investigated superlattices are listed in Table I. The fabrication and structural characterization of the superlattices have been reported in detail recently[27,29,42] and are therefore discussed only briefly here. We have used HAXRD, LAXRR, and rocking curve measurements for structural characterization of the superlattices. Figure 1 shows typical LAXRR data. Clearly, superlattice

TABLE I. Relevant parameters of the investigated $[La_{2/3}(Ca \text{ or } Ba)_{1/3}MnO_3/SrTiO_3]\times N$ superlattices fabricated on $SrTiO_3$ and $NdGaO_3$ substrates. Also shown are data for single-layer films and bulk material.

d_2 (LCMO) (nm)	d_1 (STO) (nm)	d_2 (LBMO) (nm)	N	T_p (K)	c (Å)
		on $SrTiO_3$ substrate			
		Bulk		340	3.910
		100		327	3.916
	4.7	9.5	5	318	3.923
	9.5	6.3	5	317	3.924
7.03	11.35		7	102	3.796
10.45	10.72		6	121	3.811
14.33	11.35		5	136	3.801
17.39	10.57		3	152	3.795
		on $NdGaO_3$ substrate			
	9.5	3.2	7	273	3.930
	11.3	6.0	5	304	3.936
	9.5	9.5	5	300	3.947
	9.5	6.3	5	294	3.934
	4.7	6.3	7	264	3.952
	4.7	9.5	6	204	3.975
		16		207	3.974
7.64	11.65		7	194	3.822
11.96	11.42		6	208	3.833
16.62	11.47		5	218	3.838
18.08	9.64		3	262	3.86(7)

Bragg peaks up to very high order and finite-size peaks are observed. From the LAXRR measurements a small interface roughness of only a few angstrom was derived.[27,29] Rocking curve measurements yield a small mosaic spread of 0.02° to 0.04° limited by the substrate quality.[27,29] Off-specular XRR measurements indicate that the interface roughness detected

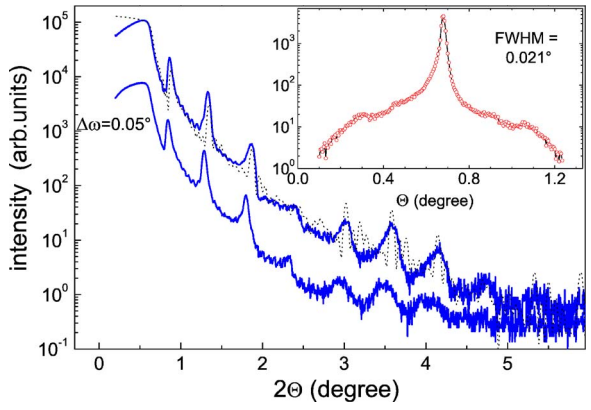

FIG. 1. (Color online) Low-angle XRR data for a $[LCMO(3.80\text{ nm})/STO(11.21\text{ nm})]_8$ superlattice on NGO. The upper line represents the specular XRR, the dotted line the fit to the data. The displaced, lower line is off-specular XRR data obtained for an offset angle of 0.05°. The inset shows the rocking curve for second-order superlattice Bragg peak.

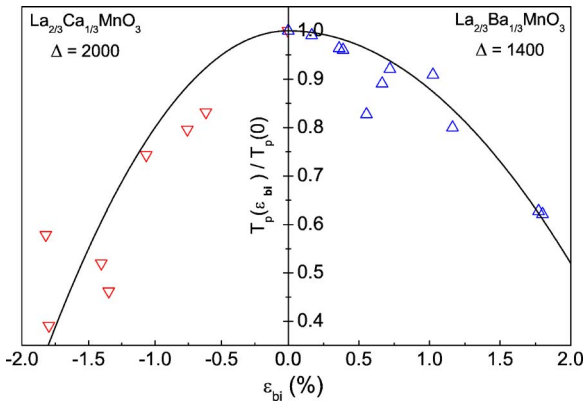

FIG. 2. (Color online) Metal-to-insulator transition temperature T_p vs biaxial distortion ε_{bi}.

by specular XRR is to a large extent correlated in the growth direction.[29] This point is confirmed by the observation of a significant diffuse background in the rocking curves due to vertically correlated roughness (see the inset of Fig. 1). The structural analysis shows that the superlattices have excellent epitaxial quality[27,29,42] and are coherently strained, allowing for the continuous variation of the biaxial strain.

By HAXRD the out-of-plane or *c*-axis lattice parameter is determined from the position of the (002) peaks of the $La_{2/3}$(Ca or Ba)$_{1/3}MnO_3$ layers (see Table I). The derived values depend on the thickness ratio d_2/d_1. In general, the *c*-axis lattice parameter approaches the bulk value on increasing d_2/d_1 except for the LCMO/STO superlattices grown on STO substrates, where *c* depends only weakly on d_2/d_1 due to the large lattice mismatch to the substrate. The deviation of the *c*-axis lattice parameter from the bulk value reflects the effect of the biaxial strain within the *ab* plane. The tensile (or compressive) strain within the *ab* plane results in a compression (expansion) of the *c* axis. Note that this results in a tetragonal or JT-type distortion that is expected to strongly affect the magnetic and electronic properties of the manganite layers. Assuming a Poisson ratio of $\nu = 0.5$, a biaxial or tetragonal distortion ε_{bi} can be derived,[27]

$$\varepsilon_{bi} = \frac{1}{4}(2\varepsilon_{zz} - \varepsilon_{xx} - \varepsilon_{yy}). \quad (1)$$

Here, $\varepsilon_{xx} = \varepsilon_{yy}$ and ε_{zz} are the in-plane and out-of-plane stress components obtained from the measured lattice parameters, respectively.

In Fig. 2 we have plotted ε_{bi} vs the temperature T_p corresponding to the peak in the resistivity vs temperature curves. It is evident that there is a similar dependence of T_p on ε_{bi} both for LBMO (tensile strain: $\varepsilon_{bi} < 0$) and LCMO (compressive strain: $\varepsilon_{bi} > 0$). From the experimental data the quantity

$$\Delta = \frac{1}{T_p}\frac{d^2T_p}{d\varepsilon_{bi}^2} \quad (2)$$

can be determined as $\Delta \simeq 1.4 \times 10^3$ and 2.0×10^3 for LBMO and LCMO, respectively. In a theoretical analysis by Millis *et al.*,[3] Δ was related to the dimensionless electron-phonon coupling $\lambda = g^2/(\kappa t)$, where *g* is the electron-phonon coupling, κ the phonon stiffness, and *t* the mean hopping amplitude. We note that the value of Δ determined in our experiments agrees well with that derived for $La_{0.83}Sr_{0.17}MnO_3$ using a resonant ultrasound method.[55] However, the experimental values are significantly smaller than the theoretical prediction.[3] The fact that Δ is larger for LCMO than for LBMO may be related to the smaller ionic radius of Ca resulting in a smaller tolerance factor. The high sensitivity of T_p on ε_{bi} implies that JT-type lattice distortions are strongly affecting the magnetotransport properties of doped manganites. We note that, in contrast to biaxial strain, compressive bulk strain (e.g., in hydrostatic pressure experiments) increases T_p.[56] This is due to the fact that uniform compression results in an increase of the electron hopping amplitude and thereby reduces the relative importance of the electron-lattice coupling. In contrast, the biaxial distortion increases the JT splitting of the e_g levels, thereby increasing the tendency of the electrons to become localized,[3] i.e., T_p is expected to decrease with increasing ε_{bi} in agreement with our data. Our systematic study on the effect of biaxial strain (both tensile and compressive) clearly demonstrates the importance of the electron-lattice coupling in the doped manganites as theoretically predicted by Millis *et al.*[3]

We also would like to address the influence of interface effects on the observed variation of T_p with biaxial strain ϵ_{bi}, since localization effects have been suggested to occur at manganite/insulator interfaces. For example, in some experiments a strong suppression of T_p accompanied by a decrease of the magnetic moment and an increase of resistance at low temperature was found for ultrathin films below about 20 nm. This has been usually interpreted as due to the presence of a magnetic dead layer with a thickness of the order of a few nanometers located at the film/substrate interface.[8,14] Recently, an interface-induced phase separation due to the breakup of the Mn-O chains and a modification in Mn^{4+}/Mn^{3+} ratio at manganite/insulator interfaces has been proposed,[26] where the disorder arising from the coexistence of different atomic terminations at the interfaces may play an important role. In our superlattices all individual manganite layers are thinner than 20 nm. The variations of T_p are dominated by variations of the biaxial strain, whereas interface effects seem to play a minor role. This is seen from the data listed in Table I. For example, the superlattices [LBMO(9.5 nm)/STO(4.7 nm)]$_5$ and [LBMO(6.3 nm)/STO(9.5 nm)]$_5$ as well as a 100 nm thick single LBMO film all fabricated on STO substrates have almost the same T_p of about 320 K. We attribute this to the same strain state in the LBMO layers in these samples. If interface effects played an important role, we would expect a considerably reduced T_p for the superlattice with only 6.3 nm thick layers. The same argument holds comparing the superlattices [LBMO(3.2 nm)/STO(9.5 nm)]$_7$ and [LBMO(9.5 nm)/STO(4.7 nm)]$_6$ fabricated on NGO substrates. The superlattice with the larger LBMO layer has the smaller T_p due to the larger biaxial strain (204 K compared to 273 K). Again, if interface effects played a dominant role, we would expect a strongly reduced T_p for the 3.2 nm thin LBMO layers. In contrast, even for this very thin LBMO layer a T_p value is observed which is

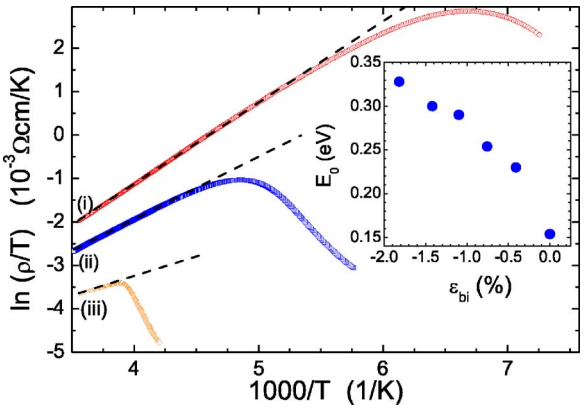

FIG. 3. (Color online) $\ln(\rho/T)$ vs $1/T$ for different superlattices: (i) $[\mathrm{LCMO}(18.08\ \mathrm{nm})/\mathrm{STO}(9.64\ \mathrm{nm})]_3$ on NGO (E_a=0.077 eV, $\varepsilon_{\mathrm{bi}}\simeq 0$); (ii) $[\mathrm{LCMO}(11.96\ \mathrm{nm})/\mathrm{STO}(11.42\ \mathrm{nm})]_6$ on NGO (E_a=0.127 eV, $\varepsilon_{\mathrm{bi}}$=−0.76%); and (iii) $[\mathrm{LCMO}(17.39\ \mathrm{nm})/\mathrm{STO}(10.57\ \mathrm{nm})]_3$ on STO (E_a=0.164 eV, $\varepsilon_{\mathrm{bi}}$=−1.82%). The dependence of the polaron binding energy $E_0\approx 2E_a$ on $\varepsilon_{\mathrm{bi}}$ is shown in the inset.

only slightly reduced below that expected according to the detected strain state. This slight reduction for the thinnest layer actually is most likely related to interface effects. The fact that interface effects play only a minor role in the investigated superlattices may be related to their high structural and interface quality, which has been confirmed both by high-resolution transmission electron microscopy and x-ray diffraction.[13,27,29] In concluding the discussion of interface effects, we can state that in the investigated superlattices biaxial strain is the dominant effect in determining T_p. In order to definitely determine the minor influence of interface effects the study of transport properties of superlattices with varying manganite layer thickness, however with the same strain state, would be required.

We next discuss the transport properties of the strained manganites films for $T>T_p$. Along the line of discussion given above, strong polaronic effects are expected. Emin and Holstein calculated the resistivity due to small polaron hopping in the adiabatic limit to[57]

$$\rho = AT\exp\left(\frac{E_a}{k_BT}\right), \quad \text{where } A=\frac{2k_B}{3ne^2a^2\nu}. \tag{3}$$

Here, n is the concentration of polarons, a the site-to-site hopping distance, ν the attempt frequency (frequency of the longitudinal optical phonon), and E_a is the activation energy, i.e., the potential barrier for polaron hopping. The activation energy consists of two terms, $E_a=E_0/2-t$, where E_0 denotes the polaron binding energy and t the overlap integral of wave functions on two lattice sites. In most cases t is negligible and $E_a\simeq E_0/2$.[58]

In Fig. 3 we have plotted $\ln(\rho/T)$ vs $1/T$ for three representative samples with different amount of the biaxial strain. It can be seen that the measured $\rho(T)$ curves can be well fitted by the small polaron model above T_p. A linear fit of the data for $T>T_p$ gives E_a. Figure 3 shows that E_a increases from 0.077 eV for an almost strain-free film to 0.127 eV for $\varepsilon_{\mathbf{bi}}$=−0.76% and further on to 0.164 eV for $\varepsilon_{\mathbf{bi}}$=−1.82%. Here, the E_a value for the strain-free film is very close to E_a=0.073 eV found for single crystals.[59] That is, E_a increases with increasing biaxial distortion. This implies that the increasing JT-type lattice distortion is primarily responsible for the increasing E_0 in the strained manganite layers. The strong JT electron-phonon coupling increases the tendency of the electrons to become localized, thereby increasing the resistivity and decreasing T_p as predicted by theory.[3]

We next address the temperature dependence of the resistivity well below T_p, that is, in the metallic phase. It has been shown[59,60] that the measured $\rho(T)$ curves of manganite thin films and bulk material can be well explained by a dependence following $\rho=\rho_0+\rho_2T^2+\rho_{4.5}T^{4.5}$, where ρ_0 is due to impurity, defect, or grain boundary scattering, the T^2 term due to electron-electron and the $T^{4.5}$ term due to electron-magnon scattering.[61] However, the $\rho(T)$ curves of the strained films could not be fitted to the above expression due to the existence of an upturn in the $\rho(T)$ curves or an almost T-independent resistivity below about 20 K (see Fig. 4). In order to fit the data we have to add a $T^{1/2}$ term, giving

$$\rho=\rho_0+\rho_2T^2+\rho_{4.5}T^{4.5}+aT^{1/2}. \tag{4}$$

Here, the appearance of the unusual $T^{1/2}$ term can be attributed to Coulomb interaction between the carriers strongly

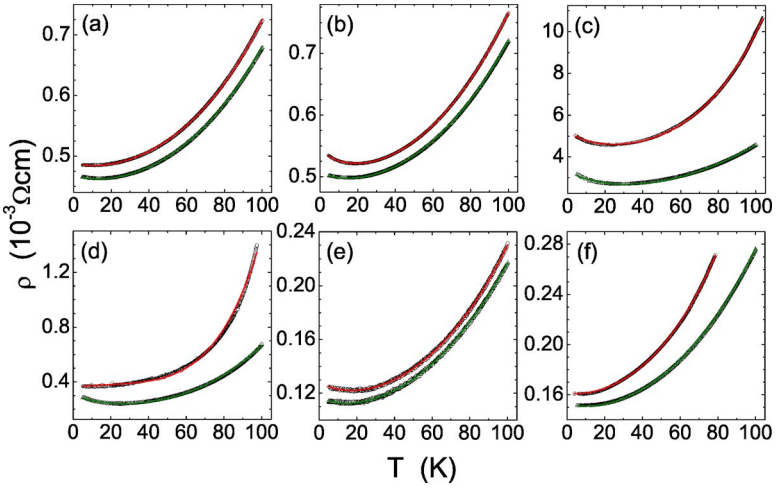

FIG. 4. (Color online) Resistivity vs temperature at H=0 and 5 T for (a) 100 nm thick LBMO film on STO ($\varepsilon_{\mathrm{bi}}$=0.17%); (b) $[\mathrm{LBMO}(9.5\ \mathrm{nm})/\mathrm{STO}(4.7\ \mathrm{nm})]_5$on STO ($\varepsilon_{\mathrm{bi}}$=0.36%); (c) the 16 nm thick LBMO film on NGO ($\varepsilon_{\mathrm{bi}}$=−1.77%); (d) $[\mathrm{LCMO}(17.39\ \mathrm{nm})/\mathrm{STO}(10.57\ \mathrm{nm})]_3$ on STO ($\varepsilon_{\mathrm{bi}}$=−1.82%); (e) $[\mathrm{LCMO}(18.08\ \mathrm{nm})/\mathrm{STO}(9.64\ \mathrm{nm})]_3$ on NGO ($\varepsilon_{\mathrm{bi}}\simeq 0$); and (f) the 40 nm thick LCMO film on NGO ($\varepsilon_{\mathrm{bi}}\simeq 0$). The solid lines are the fits to $\rho=\rho_0+\rho_2T^2+\rho_{4.5}T^{4.5}+aT^{1/2}$.

enhanced by disorder.[62] Such a term has been observed in disordered metallic systems, where its coefficient was found to change sign as a function of disorder.[62] We suggest that the JT-type lattice distortion is responsible for this term in the highly strained films.

It is striking that the $\rho(T)$ curves of samples with different amount of strain could be fitted well by Eq. (4) both for zero and high magnetic field as shown by Fig. 4. We note that in the high-quality epitaxial films the conductivity anomaly cannot be ascribed to extrinsic effects such as grain boundaries.[63–65] Figure 4 shows that the almost strain-free sample [Fig. 4(a), $\varepsilon_{bi}=0.17\%$] shows a very flat $\rho(T)$ curve below 20 K at $H=0$ and 5 T. For a weakly [Fig. 4(b), $\varepsilon_{bi}=0.36\%$] and highly strained LBMO film [Fig. 4(c), $\varepsilon_{bi}=1.77\%$] the resistivity upturn below 20 K is pronounced at $H=0$. However, for $H=5$ T the resistivity upturn of the former is significantly suppressed, whereas it is almost unchanged for the latter. For a further strained sample [Fig. 4(d), $\varepsilon_{bi}=-1.82\%$] the zero-field $\rho(T)$ is found to be very flat, whereas for $H=5$ T a clear resistivity upturn is obtained. Finally, for the almost strain-free samples [Figs. 4(e) and 4(f)], both for $H=0$ and 5 T a flat $\rho(T)$ curve is found. The different behavior of the samples with different amount of biaxial strain most likely is caused by the competition of the field-independent (ρ_0, $T^{1/2}$, and T^2 term) and field-dependent ($T^{4.5}$ term) contributions to the resistivity. Our data suggest that the strain-induced lattice distortion causes enhanced Coulomb interaction ($a<0$) and, in turn, in the observed minimum in the $\rho(T)$ curves. We note that tunneling between antiferromagnetically coupled grains as a possible origin of the resistivity upturn can be excluded, since in this case the resistivity minimum should be suppressed by anapplied magnetic field.[66]

Fitting low-temperature resistivity data by Eq. (4), we could study the variation of the parameters ρ_2 and $\rho_{4.5}$ as a function of the applied magnetic field. The parameter $\rho_{4.5}$ was found to decrease by more than 25% in a field of 5 T, whereas ρ_2 stayed about the same in most cases. Such behavior could be expected if electron-magnon scattering is suppressed by the applied magnetic field. Moreover, the ratio $\rho_{4.5}/\rho_0$ was found to show a clear decay with increasing T_p in zero magnetic field. Within the theory of low-temperature resistivity of half-metallic ferromagnets,[67] the coefficient $\rho_{4.5}$ is predicted to be inversely proportional to the square of the spin stiffness. The observed change of $\rho_{4.5}/\rho_0$ with T_p might suggest that there exists an about-linear relationship between the spin stiffness and T_p in doped manganites. However, this qualitative finding has to be confirmed by more detailed experiments. We would like to point out that our data could not be reasonably fitted by $\rho(T)=\rho_0+bT^{\alpha}+aT^{1/2}$ with $\alpha=2$, 3, 4.5, or 5. Only a combination of electron-electron scattering and electron-magnon scattering together with the $T^{1/2}$ dependence from the disorder-induced Coulomb interaction can explain our low-temperature resistivity data.

We finally discuss the magnetoresistance $\mathrm{MR}=-[R(H)-R(0)]/R(H)]$ of the strained manganite films around T_p. In Fig. 5 we have plotted MR vs T_p of the strained films together with the data of various perovskite manganites of

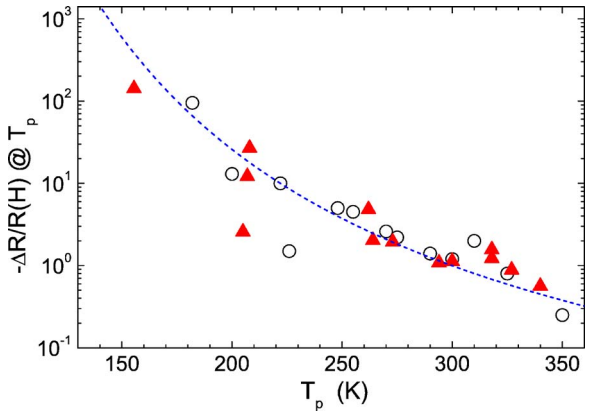

FIG. 5. (Color online) Magnetoresistance vs temperature T_p for the investigated superlattices (filled triangles). Also shown are the values of bulk samples compiled in Ref. 68 (open circles). The dotted line is a fit to $\mathrm{MR}\propto(1/T_p)\exp(E_a/k_BT_p)$ with $E_a=145$ meV.

composition $R_{1-x}D_xMnO_{3-\delta}$ compiled by Khazeni *et al.*[68] Obviously, the MR vs T_p plot follows a universal line, i.e., there is a similar dependence of MR on T_p for the biaxially strained films and samples, where T_p is changed by internal pressure due to elemental substitution. The generic decrease of MR with increasing T_p has a straightforward explanation: The difference in resistivities between the metallic and insulating regime decreases with increasing temperature. If one assumes that $\rho(T)\propto T\exp(E_a/k_BT)$ above T_p and $\rho(T)\propto T^2$ below T_p one expects $\mathrm{MR}\propto\frac{1}{T_p}\exp(E_a/k_BT_p)$(dotted line in Fig. 5). Indeed, the experimental data are close to this rough estimate. However, deviations from this estimate are also obvious, since the activation energy E_a is not constant as discussed above.

IV. CONCLUSION

In summary, we have grown high-quality $[La_{2/3}(Ca\text{ or }Ba)_{1/3}MnO_3/SrTiO_3]\times N$ superlattices with different modulation periods using L-MBE. The biaxial strain (tensile and compressive) and, in turn, the tetragonal lattice distortion could be varied over a wide range by varying the thickness ratio of the constituent layers. Our analysis shows that T_p decreases strongly with increasing biaxial distortion as $T_p/T_p(0)=1-\frac{1}{2}\Delta\varepsilon_{bi}^2$ both for tensile and compressive strain, with Δ of the order of 1500. The MR is found to increase with decreasing T_p following a universal dependence. We also show that the JT-type lattice distortions affect the magnetotransport properties in the doped manganites. An increasing distortion results in an increasing activation energy for small polaron hopping above T_p. Our results give clear evidence for the central role of JT-type lattice distortions on the physics of the CMR manganites.

ACKNOWLEDGMENTS

The authors acknowledge fruitful discussions with J. Aarts, L. Alff, M. S. Ramachandra Rao, and K. Dörr.

[1] R. von Helmolt, J. Wecker, B. Holzapfel, L. Schultz, and K. Samwer, Phys. Rev. Lett. **71**, 2331 (1993).
[2] S. Jin, T. H. Tiefel, M. McCormack, R. A. Fastnacht, R. Ramesh, and L. H. Chen, Science **264**, 413 (1994).
[3] A. J. Millis, P. B. Littlewood, and Boris I. Shraiman, Phys. Rev. Lett. **74**, 5144 (1995); see also A. J. Millis, B. I. Shraiman, and R. Mueller, *ibid.* **77**, 175 (1996); A. J. Millis, B. I. Shraiman, and R. Mueller, Nature (London) **392**, 147 (1998); and A. J. Millis, B. I. Shraiman, and R. Mueller, J. Appl. Phys. **83**, 1588 (1998).
[4] G. Zhao, K. Conder, H. Keller, and K. A. Mueller, Nature (London) **381**, 676 (1996).
[5] Amlan Biswas, M. Rajeswari, R. C. Srivastava, Y. H. Li, T. Venkatesan, R. L. Greene, and A. J. Millis, Phys. Rev. B **61**, 9665 (2000).
[6] J. Aarts, S. Freisem, R. Hendrikx, and H. W. Zandbergen, Appl. Phys. Lett. **72**, 2975 (1998).
[7] H. W. Zandbergen, S. Freisem, T. Nojima, and J. Aarts, Phys. Rev. B **60**, 10259 (1999).
[8] J. Z. Sun, D. W. Abraham, R. A. Rao, and C. B. Eom, Appl. Phys. Lett. **74**, 3017 (1999).
[9] M. Izumi, Y. Konishi, T. Nishihara, S. Hayashi, M. Shinohara, M. Kawasaki, and Y. Tokura, Appl. Phys. Lett. **73**, 2497 (1998).
[10] J. N. Eckstein, I. Bozovic, J. O'Donnell, M. Onellion, and M. S. Rzchowski, Appl. Phys. Lett. **69**, 1312 (1996).
[11] K. Dörr, J. M. de Teresa, K.-H. Müller, D. Eckert, T. Walter, E. Vlakhov, K. Nenkov, and L. Schultz, J. Phys.: Condens. Matter **12**, 7099 (2000).
[12] F. S. Razavi, G. Gross, H.-U. Habermeier, O. Lebedev, S. Amelinckx, G. Van Tendeloo, and A. Vigliante, Appl. Phys. Lett. **76**, 155 (2000).
[13] B. Wiedenhorst, C. Höfener, Y. Lu, J. Klein, L. Alff, R. Gross, B. H. Freitag, and W. Mader, Appl. Phys. Lett. **74**, 3636 (1999); see also J. Magn. Magn. Mater. **211**, 16 (2000).
[14] M. Bibes, Ll. Balcells, S. Valencia, J. Fontcuberta, M. Wojcik, E. Jedryka, and S. Nadolski, Phys. Rev. Lett. **87**, 067210 (2001).
[15] J. Zhang, H. Tanaka, T. Kanki, J. H. Choi, and T. Kawai, Phys. Rev. B **64**, 184404 (2001).
[16] T. Kanki, H. Tanaka, and T. Kawai, Phys. Rev. B **64**, 224418 (2001).
[17] M. Ziese, H. C. Semmelhack, and K. H. Han, Phys. Rev. B **68**, 134444 (2003).
[18] S. Valencia, L. I. Balcells, J. Fontcuberta, and Martinez, Appl. Phys. Lett. **82**, 4531 (2003).
[19] M. Paranjape, A. K. Raychaudhuri, N. D. Mathur, and M. G. Blamire, Phys. Rev. B **67**, 214415 (2003).
[20] Yu. A. Boikov and T. Claeson, Phys. Solid State **47**, 287 (2005); see also Tech. Phys. Lett. **30**, 535 (2004).
[21] J. Klein, J. B. Philipp, G. Carbone, A. Vigliante, L. Alff, and R. Gross, Phys. Rev. B **66**, 052414 (2002).
[22] J. Klein, J. B. Philipp, D. Reisinger, M. Opel, A. Marx, A. Erb, L. Alff, and R. Gross, J. Appl. Phys. **93**, 7373 (2003).
[23] S. Jacob, T. Roch, F. S. Razavi, G. M. Gross, and H.-U. Habermeier, J. Appl. Phys. **91**, 2232 (2002).
[24] K. H. Ahn, T. Lookman, and A. R. Bishop, Nature (London) **428**, 401 (2004).
[25] Z. Q. Yang, R. Hendrikx, J. Aarts, Y. L. Qin, and H. W. Zandbergen, Phys. Rev. B **70**, 174111 (2004).
[26] F. Giesen, B. Damaschke, V. Moshnyaga, K. Samwer, and G. A. Müller, Phys. Rev. B **69**, 014421 (2004).
[27] Yafeng Lu, J. Klein, C. Hoefener, B. Wiedenhorst, J. B. Philipp, F. Herbstritt, A. Marx, L. Alff, and R. Gross, Phys. Rev. B **62**, 15806 (2000).
[28] Moon-Ho Jo, Neil D. Mathur, Jan E. Evetts, Mark G. Blamire, Manuel Bibes, and Josep Fontcuberta, Appl. Phys. Lett. **75**, 3689 (1999).
[29] Yafeng Lu, J. Klein, F. Herbstritt, J. B. Philipp, A. Marx, L. Alff, and R. Gross, Phys. Status Solidi B **242**, 1545 (2005).
[30] Land J. Belenky, Xianglin Ke, Mark Rzchowski, and C. B. Eom, J. Appl. Phys. **97**, 10J107 (2005).
[31] P. Reutler, A. Bensaid, F. Herbstritt, C. Höfener, A. Marx, and R. Gross, Phys. Rev. B **62**, 11619 (2000).
[32] A. Marx, J. B. Philipp, P. Reutler, A. Bensaid, F. Herbstritt, C. Höfener, and R. Gross, in *Proceedings of the 16th International Conference on Noise in Physical Systems and 1/f Fluctuations ICNF 2001*, Gainesville, FL, edited by G. Bosman (World Scientific, Singapore, 2001), pp. 31–34.
[33] H. T. Hardner, M. B. Weissman, M. Jaime, R. E. Treece, P. C. Dorsey, J. S. Horwitz, and D. B. Chrisey, J. Appl. Phys. **81**, 272 (1997).
[34] R. D. Merithew, M. B. Weissman, F. M. Hess, P. Spradling, E. R. Nowak, J. O'Donnell, J. N. Eckstein, Y. Tokura, and Y. Tomioka, Phys. Rev. Lett. **84**, 3442 (2000).
[35] B. Raquet, A. Anane, S. Wirth, P. Xiong, and S. von Molnar, Phys. Rev. Lett. **84**, 4485 (2000).
[36] F. M. Hess, R. D. Merithew, M. B. Weissman, Y. Tokura, and Y. Tomioka, Phys. Rev. B **63**, 180408(R) (2001).
[37] A. Palanisami, R. D. Merithew, M. B. Weissman, and J. N. Eckstein, Phys. Rev. B **64**, 132406 (2001).
[38] A. Palanisami, M. B. Weissman, and N. D. Mathur, Phys. Rev. B **71**, 094419 (2005).
[39] J. W. Matthews, J. Vac. Sci. Technol. **12**, 126 (1975).
[40] A. Biswas, M. Rajeswari, R. C. Srivastava, T. Venkatesan, R. L. Greene, Q. Lu, A. L. de Lozanne, and A. J. Millis, Phys. Rev. B **63**, 184424 (2001).
[41] A. Biswas, M. Rajeswari, R. C. Srivastava, Y. H. Li, T. Venkatesan, R. L. Greene, and A. J. Millis, Phys. Rev. B **61**, 9665 (2000).
[42] R. Gross, J. Klein, B. Wiedenhorst, C. Höfener, U. Schoop, J. B. Philipp, M. Schonecke, F. Herbstritt, L. Alff, Yafeng Lu, A. Marx, S. Schymon, S. Thienhaus, and W. Mader, in *Superconducting and Related Oxides: Physics and Nanoengineering IV*, edited by D. Pavuna and I. Bosovic, SPIE Conference Proceedings (SPIE, Bellingham, WA, 2000), Vol. 4058, pp. 278–294.
[43] M. Jaime, M. B. Salamon, M. Rubinstein, R. E. Treece, J. S. Horwitz, and D. B. Chrisey, Phys. Rev. B **54**, 11914 (1996).
[44] M. Jaime, H. T. Hardner, M. B. Salamon, M. Rubinstein, P. Dorsey, and D. Emin, Phys. Rev. Lett. **78**, 951 (1997).
[45] D. C. Worledge, L. Mieville, and T. H. Geballe, Phys. Rev. B **57**, 15267 (1998).
[46] M. Ziese and C. Srinitiwarawong, Phys. Rev. B **58**, 11519 (1998).
[47] Wontae Chang, Steven W. Kirchoefer, Jeffrey M. Pond, Jeffrey A. Bellotti, Syed B. Qadri, Jeffrey H. Haeni, and Darrell G. Schlom, J. Appl. Phys. **96**, 6629 (2004).
[48] J. H. Haeni, P. Irvin, W. Chang, R. Uecker, P. Reiche, Y. L. Li, S. Choudhury, W. Tian, M. E. Hawley, B. Craigo, A. K. Tagantsev, X. Q. Pan, S. K. Streiffer, L. Q. Chen, S. W. Kirchoefer, J. Levy, and D. G. Schlom, Nature (London) **430**, 758 (2004).
[49] H. Uwe and T. Sakudo, Phys. Rev. B **13**, 271 (1976).

[50] N. A. Pertsev, A. G. Zembilgotov, and A. K. Tagantsev, Phys. Rev. Lett. **80**, 1988–1991 (1998); see also N. A. Pertsev, A. K. Tagantsev, and A. Setter, Phys. Rev. B **61**, R825 (2000).
[51] H. Sato and M. Naito, Physica C **274**, 221 (1997).
[52] I. Bozovic, G. Logvenov, I. Belca, B. Narimbetov, and I. Sveklo, Phys. Rev. Lett. **89**, 107001 (2002).
[53] J. Klein, C. Höfener, L. Alff, and R. Gross, Supercond. Sci. Technol. **12**, 1023 (1999).
[54] J. Klein, C. Höfener, L. Alff, and R. Gross, J. Magn. Magn. Mater. **211**, 9 (2000).
[55] T. W. Darling, A. Migliori, E. G. Moshopoulou, S. A. Trugman, J. J. Neumeier, J. L. Sarrao, A. R. Bishop, and J. D. Thompson, Phys. Rev. B **57**, 5093 (1998).
[56] H. Y. Hwang, T. T. M. Palstra, S-W. Cheong, and B. Batlogg, Phys. Rev. B **52**, 15046 (1995).
[57] D. Emin and T. Holstein, Ann. Phys. (N.Y.) **53**, 439 (1969).
[58] N. F. Mott and E. A. Davis, *Electronic Processes in Non-crystalline Materials* (Clarendon, Oxford, 1971).
[59] G. J. Snyder, R. Hiskes, S. DiCarolis, M. R. Beasley, and T. H. Geballe, Phys. Rev. B **53**, 14434 (1996).
[60] S. V. Pietambaram, D. Kumar, R. V. Singh, C. B. Lee, and V. S. Kaushik, J. Appl. Phys. **86**, 3317 (1999).
[61] K. Kubo and N. Ohata, J. Phys. Soc. Jpn. **33**, 21 (1972).
[62] P. A. Lee and T. V. Ramkrishnan, Rev. Mod. Phys. **57**, 287 (1985).
[63] J. Klein, C. Höfener, S. Uhlenbruck, L. Alff, B. Büchner, and R. Gross, Europhys. Lett. **47**, 371 (1999).
[64] R. Gross, L. Alff, B. Büchner, B. H. Freitag, C. Höfener, J. Klein, Yafeng Lu, W. Mader, J. B. Philipp, M. S. R. Rao, P. Reutler, S. Ritter, S. Thienhaus, and S. Uhlenbruck, J. Magn. Magn. Mater. **211**, 150 (2000).
[65] C. Höfener, J. B. Philipp, J. Klein, L. Alff, A. Marx, B. Büchner, and R. Gross, Europhys. Lett. **50**, 681 (2000).
[66] E. Rozenberg, M. Auslender, I. Felner, and G. Gorodetsky, J. Appl. Phys. **88**, 2578 (2000); **89**, 6639 (2001).
[67] K. Kubo and N. A. Ohata, J. Phys. Soc. Jpn. **33**, 21 (1972).
[68] K. Khazeni, Y. X. Jia, Li Lu, Vincent H. Crespi, Marvin L. Cohen, and A. Zettl, Phys. Rev. Lett. **76**, 295 (1996).